

A Minimal Model for Carnot Efficiency at Maximum Power

Shiling Liang (梁师翎)^{1,2,*} Yu-Han Ma,^{3,4,†} Daniel Maria Busiello,⁵ and Paolo De Los Rios^{1,6}

¹*Institute of Physics, School of Basic Sciences, École Polytechnique Fédérale de Lausanne (EPFL), 1015 Lausanne, Switzerland*

²*Biological Complexity Unit, Okinawa Institute of Science and Technology Graduate University, Onna, Okinawa 904-0495, Japan*

³*Department of Physics, Beijing Normal University, Beijing, 100875, China*

⁴*Graduate School of China Academy of Engineering Physics,*

No. 10 Xibeiwang East Road, Haidian District, Beijing, 100193, China

⁵*Max Planck Institute for the Physics of Complex Systems, 01187 Dresden, Germany*

⁶*Institute of Bioengineering, School of Life Sciences,*

École Polytechnique Fédérale de Lausanne (EPFL), 1015 Lausanne, Switzerland

Carnot efficiency sets a fundamental upper bound on the heat engine efficiency, attainable in the quasi-static limit, albeit at the cost of completely sacrificing power output. In this Letter, we present a minimal heat engine model that can attain Carnot efficiency while achieving maximum power output. We unveil the potential of intrinsic divergent physical quantities within the working substance, such as degeneracy, as promising thermodynamic resources to break through the universal power-efficiency trade-off imposed by nonequilibrium thermodynamics for conventional heat engines. Our findings provide novel insights into the collective advantage in harnessing energy of many-body interacting systems.

Introduction.— Heat engines generally operate between two thermal baths at different temperatures ($T_h > T_c$), converting thermal energy into output work. The efficiency of a heat engine, $\eta = W/Q_h$, given by the ratio of the output work W to the absorbed heat Q_h , is bounded by the second law of thermodynamics [1], with the upper limit defined by the Carnot efficiency $\eta_C = 1 - T_c/T_h$. The Carnot limit is reached when the engine operates in the quasi-static regime, resulting in zero output power. However, achieving both high efficiency and finite power is crucial for practical applications. To evaluate the performance of finite-time heat engines, efficiency at maximum power (EMP) [2–7] and trade-off relations between power and efficiency [8–12] were proposed as typical benchmarks and attracted significant attention in the fields of nonequilibrium thermodynamics and engineering thermodynamics [13, 14].

In contrast to the limitations imposed by universal power-efficiency trade-offs [8–11] on conventional heat engines, recent studies have revealed intriguing possibilities in achieving Carnot efficiency with finite power [15–18] or even maximum power [19, 20] by utilizing working substance with intrinsic divergent physical quantities. This achievement is attributed to the scaling behavior of many-body interacting systems. These remarkable findings [15–20] not only offer a viable pathway for enhancing heat engine performance but also raise a challenging problem regarding the quantification of performance for unconventional heat engines: Do heat engines with divergent physical quantities still exhibit a trade-off relation between power and efficiency?

To shed light on this problem, we present a minimal model (schematically depicted in Fig. 1a) that incorporates intrinsic energy level degeneracy, thereby circumventing the complexity while capturing the basic de-

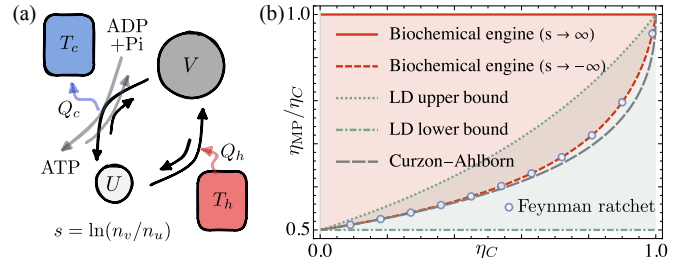
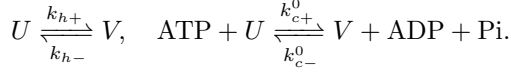


FIG. 1. (a) A biochemical engine that synthesizes ATP by operating between two thermal baths. U and V are two coarse-grained states with degeneracies n_u and n_v . (b) The EMP can go beyond the universal upper bound of the low-dissipation (LD) engines [7] and reach Carnot efficiency at $s \rightarrow \infty$.

generate characteristics arising from many-body interaction. This particular engine demonstrates the ability to achieve Carnot efficiency at maximum power (see Fig. 1b). More importantly, we analytically derive the asymptotic behavior of the power-efficiency trade-off relation (Fig. 2f) in the limit of large degeneracy of the high-energy state and explicitly demonstrate the violation of the $1/2$ -universality of EMP [4, 21] in the thermodynamic limit (see Fig. 3). We show that the thermodynamic advantage of the proposed engine stems from the first-order phase transition occurring far from the linear response regime.

Model.— We consider a biochemical engine composed of a low-energy state U and a high-energy state V representing two coarse-grained states with n_u and n_v microscopic conformations, respectively (see Fig. 1a). For example, U and V can represent the folded and unfolded states of a polymer [22, 23] or chemical species [24]. Their entropy difference is $s = \ln(n_u/n_v)$. There are two reaction paths between U and V : ATP-hydrolysis-driven

reaction under low temperature T_c , and a spontaneous transition coupled to high-temperature reservoir T_h ,



Here $\{k_{c+}^0, k_{c-}^0\}$ denote the forward and backward ATP-driven reactions, and $\{k_{h+}, k_{h-}\}$ are the high-temperature induced transitions. Absorbing the chemostatted concentrations of ATP and ADP into the rates, we can define effective non-equilibrium transition rates $k_{c+} = k_{c+}^0[\text{ATP}]$ and $k_{c-} = k_{c-}^0[\text{ADP}][\text{Pi}]$. All rates must satisfy local detailed balance, $k_{h-}/k_{h+} = e^{\beta_h \epsilon_h - s}$ and $k_{c-}/k_{c+} = e^{\beta_c \epsilon_c - s}$, where $\beta = 1/k_B T$ [25, 26]. The energy gap $\Delta\mu \equiv \epsilon_h - \epsilon_c$ is the output work per cycle in terms of ATP synthesis.

The dynamics of the system is described by the master equation

$$\begin{aligned} \frac{d}{dt} p_u &= (k_{h-} + k_{c-}) p_v - (k_{h+} + k_{c+}) p_u, \\ \frac{d}{dt} p_v &= (k_{h+} + k_{c+}) p_u - (k_{h-} + k_{c-}) p_v. \end{aligned} \quad (1)$$

where p_u and p_v are the probabilities of two states. Each reaction path has a corresponding equilibrium distribution, i.e., $\pi_u^h/\pi_v^h = k_{h-}/k_{h+}$ and $\pi_u^c/\pi_v^c = k_{c-}/k_{c+}$. With normalization condition,

$$\pi_v^{h/c} = \frac{1}{1 + e^{\beta_{h/c} \epsilon_{h/c} - s}}, \quad \pi_u^{h/c} = \frac{e^{\beta_{h/c} \epsilon_{h/c} - s}}{1 + e^{\beta_{h/c} \epsilon_{h/c} - s}}. \quad (2)$$

At stationarity, $p_{u/v}^{\text{ss}} = (\tau_h \pi_{u/v}^c + \tau_c \pi_{u/v}^h) / (\tau_h + \tau_c)$ as a consequence of the competition between two reaction paths with typical time-scales $\tau_h = (k_{h+} + k_{h-})^{-1}$ and $\tau_c = (k_{c+} + k_{c-})^{-1}$. The corresponding steady-state cyclic current is [27]

$$J^{\text{ss}} = \tau^{-1} (\pi_v^h - \pi_v^c), \quad (3)$$

where $\tau = \tau_h + \tau_c$ is the characteristic time of completing the cycle. The change of internal entropy does not lead to entropy production into the environment [26, 28, 29], and thus the heat absorption rate from the hot (cold) reservoir is given by $\dot{Q}_h = J^{\text{ss}} \epsilon_h$ ($\dot{Q}_c = -J^{\text{ss}} \epsilon_c$). The steady-state output power is

$$P = J^{\text{ss}} (\epsilon_h - \epsilon_c) = \tau^{-1} (\pi_v^h - \pi_v^c) (\epsilon_h - \epsilon_c), \quad (4)$$

then the thermodynamic efficiency reads

$$\eta = P/\dot{Q}_h = 1 - (\epsilon_c/\epsilon_h). \quad (5)$$

One can find that the quasi-static limit, i.e. $J^{\text{ss}} = 0$, is reached when $\epsilon_c T_h = \epsilon_h T_c$ and leads to Carnot efficiency.

Optimization of the engine.— To maximize the power of the biochemical engine, we set the entropy difference s as a control parameter and optimize the two energy levels

ϵ_c and ϵ_h under different T_h and T_c . For convenience, we set $k_B T_h = 1$ as the reference energy. We follow the convention to assume the characteristic time τ constant because it is a kinetic parameter and thus not constrained by thermodynamics in general cases [6]. Therefore, we optimize the work of the thermodynamic cycle,

$$W = \tau P = (\pi_v^h - \pi_v^c) (\epsilon_h - \epsilon_c) \equiv W_{\text{Otto}}. \quad (6)$$

This function has an intuitive geometric representation in the phase space, as shown in Fig. 2a. Indeed, it corresponds to the work of an Otto cycle $abcd$ operating between two thermal reservoirs. Hereafter, we rescale physical quantities by s , i.e., $\bar{x} \equiv x/s$. In the Otto cycle, the two quench processes $d \rightarrow a$ and $b \rightarrow c$ do not have intrinsic speed limit while the two isothermal relaxations $c \rightarrow d$ and $a \rightarrow b$ have intrinsic time scales $\tau_{h/c} = k_{h/c}^{-1}$ that set $\tau = \tau_h + \tau_c$ as the time of completing the cycle.

Let us start with limiting cases. In Fig. 1b, we present EMP as a function of η_C for different s . When $s \rightarrow -\infty$, we can expand p_u^{ss} with respect to e^s , and thus the power reduces to $P = [T_c e^s (e^{-\theta(1-\eta)} - e^{-\theta(1-\eta_C)}) \eta \theta] / \tau$, where $\theta \equiv \epsilon_h \beta_c$. This expression has the same mathematical structure as Feynman's ratchet heat engine whose closed-form EMP has been obtained in [6]. The resulting EMP (blue dots in Fig. 1b) serves as the lower bound of the biochemical engine and is higher than the Curzon-Ahlborn efficiency [30].

The other limit is for large s , i.e., high degeneracy of the high-energy state. Although a closed form for EMP cannot be obtained in this case, we numerically show in Fig. 1b that η_{MP} can go beyond the universal upper bound, $\eta_C / (2 - \eta_C)$, of low-dissipation heat engines [7] and even reach the Carnot efficiency in the $s \rightarrow \infty$ limit (red solid line). In Fig. 2b, we illustrate the efficiency of the biochemical engine as a function of the thermodynamic parameters $\bar{\epsilon}_h/T_h$ and $\bar{\epsilon}_c/T_c$. The color map represents the relative deviation of efficiency from η_C , $\Delta\tilde{\eta} \equiv 1 - \eta/\eta_C$, which approaches 0 in the $s \rightarrow \infty$ limit. Points and dashed line indicate the optimal $(\bar{\epsilon}_h^*, \bar{\epsilon}_c^*)$ that maximize the power under different s . Fig. 2b and Fig. 2c together indicate that the optimization of power and efficiency coincide in the large- s limit and lead to Carnot efficiency at maximum power.

Thermodynamic advantage of phase transition.— As illustrated in Fig. 2c, in the large- s limit, the maximum power is achieved when $\bar{\epsilon}_{h/c}^*/T_{h/c} \rightarrow 1$. These optimized energy gaps correspond to the most sensitive response region of the equilibrium curves $\pi_v^{h/c}(\bar{\epsilon})$, as shown in Fig. 2d. Since their slope

$$\left. \frac{d\pi_v^{h/c}(\bar{\epsilon})}{d\bar{\epsilon}} \right|_{\bar{\epsilon}=T_{h/c}} = -\frac{s}{4T_{h/c}} \quad (7)$$

scales linearly with s , $T_{h/c} = \bar{\epsilon}_{h/c}$ are two phase-transition points in the $s \rightarrow \infty$ limit.

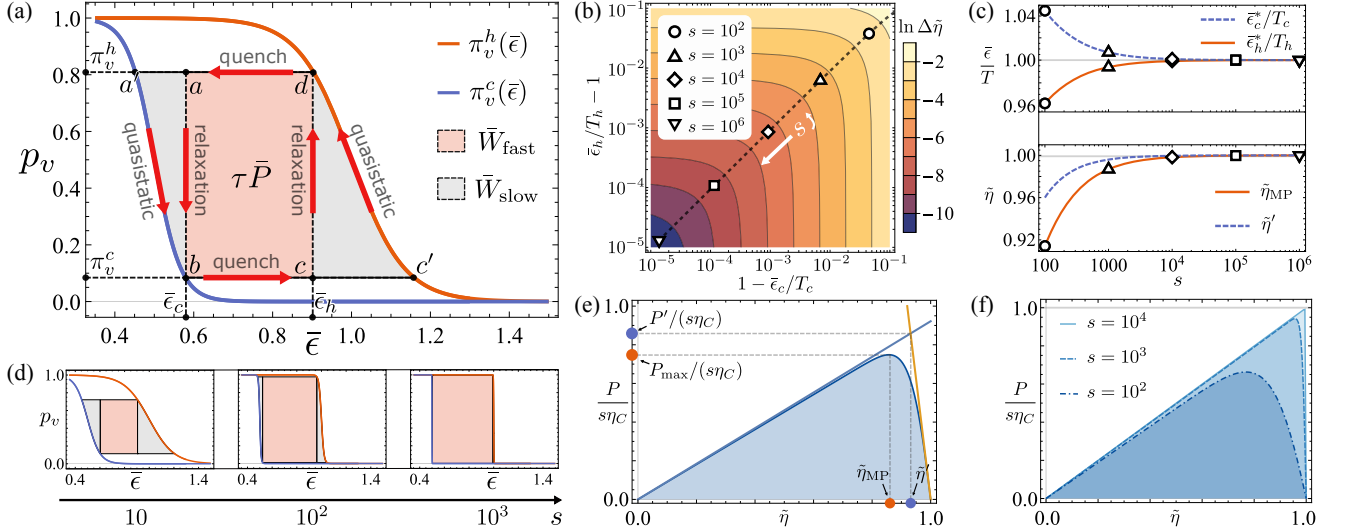


FIG. 2. Optimization of the biochemical engine. (a) An Otto cycle, $abcd$, operates between two thermal reservoirs. The red and blue curves denote the equilibrium population on state v coupled to T_h and T_c , respectively. The $a'bc'd$ cycle is a Carnot. (b) Deviation from Carnot efficiency $\Delta\tilde{\eta} = 1 - \eta/\eta_C$ as a function of thermodynamic parameters $\bar{\epsilon}_h/T_h$ and $\bar{\epsilon}_c/T_c$. The points and the dashed line indicate the optimal parameters, $\bar{\epsilon}_h^*$ and $\bar{\epsilon}_c^*$, that maximize the power for different s . (c) In the large- s limit, the maximum power is reached when $\bar{\epsilon}_{c/h}^*/T_{c/h} \rightarrow 1$ and the rescaled EMP, $\tilde{\eta}_{MP} = \eta/\eta_C$, approaches 1. (d) The Otto cycle is optimized to attain maximum work for increasing values of s . (e) The power-efficiency trade-off and the linear expansion lines from the two endpoints $\tilde{\eta} \rightarrow 0$ and $\tilde{\eta} \rightarrow 1$. The intersection of these two lines gives an upper bound of the maximum power P' , and corresponding efficiency η' . (f) The power-efficiency trade-off of the biochemical engine shows that the maximum power scales with $s\eta_C$ in the large- s limit. In the numerical optimization, we set $k_B T_h = 1$ as the reference energy and $\eta_C = 0.5$.

To provide intuition on why the phase transition enables high engine performance, we geometrically examine how thermodynamic cycles change for increasing s . The irreversible dissipation in the Otto cycle comes from the two relaxation processes. The dissipation associated with a relaxation process is given by the Kullback-Leibler divergence between the initial and final state [31, 32]. To extract the associated work, W_{slow} , one must go through the Carnot cycle $a'bc'da$ with two quasi-static processes (see Fig. 2a). Since the quality of the Otto cycle can be evaluated by comparing it with the Carnot cycle, we define the quality factor Q as the ratio of $W_{\text{Otto}} \equiv W_{\text{fast}}$ to $W_{\text{Carnot}} \equiv W_{\text{fast}} + W_{\text{slow}}$. In the $s \gg 1$ regime, we find [27]

$$Q \equiv \frac{\bar{W}_{\text{Otto}}}{\bar{W}_{\text{Carnot}}} = \frac{\bar{W}_{\text{fast}}}{\bar{W}_{\text{fast}} + \bar{W}_{\text{slow}}} \simeq \left. \frac{\bar{\epsilon}_h - \bar{\epsilon}_c}{T_h - T_c} \right|_{s \gg 1}, \quad (8)$$

which indicates that the power-optimized biochemical engine operates close to the phase transition point in both reservoirs, i.e., $T_{h/c}/\bar{\epsilon}_{h/c}^* \rightarrow 1$ (Fig. 2c). Therefore, the quality factor approaches 1 and the Otto cycle coincides with the Carnot cycle (Fig. 2d).

At this point, we conclude that the first-order phase transition induced by the divergence of high-energy level degeneracy is a favorable thermodynamic resource, allowing the EMP to approach the Carnot efficiency. Previous studies also reported the thermodynamic advantages stemming from phase transitions, but limited to cases in-

volving finite power [15] and quasi-static cycle [33]. We emphasize that our model not only distills the minimal ingredients that embody the thermodynamic advantage of phase transition but also suggests that this advantage can be maintained throughout the entire operating range of heat engines, from quasi-static to slow driving and even to fast driving.

Trade-off between power and efficiency.— The power of the engine can be written in terms of ϵ_h and the rescaled efficiency $\tilde{\eta} \equiv \eta/\eta_C$ by using Eq. (5):

$$P = \tilde{\eta} \epsilon_h \tau^{-1} \left(\frac{\eta_C}{e^{\epsilon_h - s} + 1} - \frac{\eta_C}{e^{\frac{\epsilon_h(1 - \tilde{\eta}\eta_C)}{1 - \tilde{\eta}\eta_C} - s} + 1} \right). \quad (9)$$

The power-efficiency trade-off curve [9–11, 34] is determined by $\partial_{\epsilon_h} P(\epsilon_h, \tilde{\eta}; \eta_C, s) = 0$ which can be expanded around the two ends, $\tilde{\eta} \approx 0$ and $\tilde{\eta} \approx 1$ for large values of s [27] (see Fig. 2e):

$$\begin{cases} \lim_{\tilde{\eta} \rightarrow 0} P \simeq (s - \ln s)\eta_C \tilde{\eta}, \\ \lim_{\tilde{\eta} \rightarrow 1} P \simeq \frac{s^2 \eta_C^2}{4(1 - \tilde{\eta})} (1 - \tilde{\eta}). \end{cases} \quad (10)$$

As shown in Fig. 2f, when $s \rightarrow \infty$, the shape of the trade-off curve approaches an isosceles right triangle in the rescaled parametric space.

The intersection of the two expansions in Eq. (10) (two lines in Fig. 2e) provides a good estimation of maximum

power, P' , and EMP, η' . Indeed,

$$P_{\max} \simeq P' \simeq s\eta_C, \quad \tilde{\eta}_{\text{MP}} \simeq \tilde{\eta}' \simeq 1 - \frac{4(1-\eta_C)}{s\eta_C}, \quad (11)$$

The difference between $\tilde{\eta}_{\text{MP}}$ and $\tilde{\eta}'$ decreases as s increases, and they eventually converge towards the Carnot efficiency ($\tilde{\eta} = 1$) for $s \rightarrow \infty$. We note that the EMP in Eq. (11) obtained from the power-efficiency trade-off recovers the result of Ref. [20] in which the authors found the EMP by solving the global maximum power. The power-efficiency trade-off presented in the current work provides complete performance information, such as the maximum efficiency for a given power or the maximum power for a given efficiency, for heat engines whose working substance exhibits degeneracy.

Equation (11) indicates that the maximum power scales with $s\eta_C$ while the corresponding EMP approaches Carnot efficiency with the scaling of $(s\eta_C)^{-1}$, see Fig. 2c and Fig. 2f. This scaling relation can be seen as $\lim_{s \gg 1} P_{\max} \simeq sk_B\Delta T$, where $\Delta T \equiv T_h - T_c$. For many-body interacting systems, the number of microscopic states n scales exponentially with system size N (e.g., number of interacting individuals). Since s scales as the logarithm of n , it goes linearly with N . Thus, the power of each individual, P_I , scales with $k_B\Delta T$ in the large- s regime, i.e., $P_I = P/N \sim P/s \sim k_B\Delta T$.

In a recent study [34], Shiraishi et al. proposed a universal power-efficiency trade-off as

$$P \leq \Theta \beta_c \eta_C^2 \tilde{\eta} (1 - \tilde{\eta}), \quad (12)$$

where Θ is a quantity related to state and size of the heat engine. For a finite-size heat engine, Θ remains finite, and thus the Carnot efficiency can not be reached with finite power. However, with divergent system sizes, Θ may also diverge, allowing the Carnot efficiency to be approached arbitrarily closely at maximum power. Comparing Eq. (12) with Eq. (10), we get prefactor Θ in the two limiting cases

$$\begin{cases} \Theta_0 \equiv \lim_{\tilde{\eta} \rightarrow 0} \Theta \simeq \frac{(s - \ln s)}{\eta_C \beta_c^2} \\ \Theta_1 \equiv \lim_{\tilde{\eta} \rightarrow 1} \Theta \simeq \frac{s^2}{4(1-\eta_C)\beta_c} \end{cases} \Rightarrow \frac{\Theta_1}{\Theta_0} \sim s, \quad (13)$$

illustrating that the ratio of the two prefactors scales linearly with s in the large- s limit. Note that, although we have shown the connection between the trade-off we obtained and the universal power-efficiency trade-off [34], different Θ under different limits of $\tilde{\eta}$, i.e., $\Theta_0 \neq \Theta_1$, imply that for heat engines with divergent physical quantities near the phase transition point, it is not possible to characterize the performance of the engine over the entire range of $\tilde{\eta}$ using a unified Θ . In other words, Θ is an implicit function of $\tilde{\eta}$ [35].

As a final remark, the presented results clearly demonstrate that the performance of our biochemical engine exceeds the universal power-efficiency trade-off obtained in

the low-dissipation regime [9, 10, 12]. In this regime, the trade-off relation is determined by the typical $1/t$ scaling of irreversible entropy generation [7, 10, 11, 36, 37], $S^{(\text{ir})} = \Sigma/t$, where t is proportional to cycle duration. For non-interacting systems, both Σ and the reversible entropy change, ΔS , increase with the system size [10, 11, 37]. Consequently, the only way to reduce energy dissipation is to slow down the cycle operation, resulting in higher efficiency but lower output power. However, for many-body interacting systems, the coefficient Σ can effectively be reduced by increasing the system size [18, 38], enabling high-speed cycles that achieve Carnot efficiency when $S^{(\text{ir})}/\Delta S \rightarrow 0$. This observation is consistent with our current work: in the geometric representation of the cycle, \bar{W}_{slow} and \bar{W}_{fast} respectively correspond to $S^{(\text{ir})}$ and ΔS . For a given cycle duration, the ratio $\bar{W}_{\text{slow}}/\bar{W}_{\text{fast}}$ decreases with s and eventually approaches zero in the large- s regime.

Break down the 1/2-universality of EMP.— For a heat engine operating in the linear irreversible regime ($\Delta T/T_h \ll 1$), the first-order coefficient of the EMP with respect to η_C is $1/2$ [21], a result believed to be universal in the field [4, 6, 11, 12]. However, this universality relies on the validity of linear-irreversible thermodynamics and can be violated in the presence of divergent quantities [19, 39]. Indeed, our minimal heat engine shows a violation of the 1/2-universality when $s \rightarrow \infty$ due to the divergent slope of the equilibrium population curves, as demonstrated by Eq. (7). Noticing that the order of taking $s \rightarrow \infty$ and $\eta_C \rightarrow 0$ significantly affects the result:

$$\begin{cases} \lim_{\eta_C \rightarrow 0} \lim_{s \rightarrow \infty} \eta_{\text{MP}} = \eta_C/2 \\ \lim_{s \rightarrow \infty} \lim_{\eta_C \rightarrow 0} \eta_{\text{MP}} = \eta_C. \end{cases} \quad (14)$$

This implies that, in the parametric space of η_C and s , different limit paths lead to different EMPs. By varying the limit path, the coefficient of EMP with respect to η_C transitions continuously from $1/2$ to 1 , as shown in Fig. 3a with the color map $\tilde{\eta}_{\text{MP}} \equiv \eta_{\text{MP}}/\eta_C$.

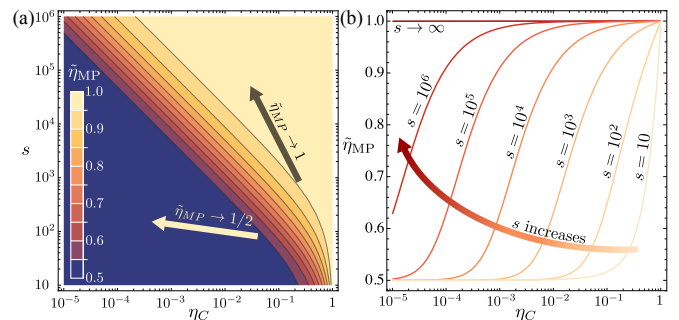


FIG. 3. (a) The rescaled EMP, $\tilde{\eta}_{\text{MP}} \equiv \eta_{\text{MP}}/\eta_C$, approaches to 1 when $s \rightarrow \infty$ faster than $\eta_C \rightarrow 0$, which breaks the 1/2-universality. (b) $\tilde{\eta}_{\text{MP}}$ as a function of η_C with different s .

For working substances of finite size, one can always choose a small enough η_C to have the corresponding EMP

approaching $\eta_C/2$ (see Fig. 3b) [27]. In this sense, the universality of $\lim_{\eta_C \rightarrow 0} \eta_{MP} = \eta_C/2$ holds in the finite-size case. As a consequence, the criterion to determine whether the proposed engine is operating in the linear irreversible regime should be $s\eta_C \ll 1$ instead of the customary $\eta_C \ll 1$.

Conclusion.— In this work, we propose a minimal model that highlights the absence of a general power-efficiency trade-off relation for heat engines with divergent quantities. The discrepancy between the EMP and Carnot efficiency is dictated by the system size, which is characterized by the number of microscopic states. Remarkably, Carnot efficiency at maximum power is attained in the thermodynamic limit with infinite system size. This observation aligns with recent findings on phase-transition-enhanced performance of heat engines [15, 40].

Our minimal model also reveals the beneficial impact on heat engine performance of engineering microscopic states to form two coarse-grained states with distinct degeneracies. These two can be regarded as ordered and disordered states during a phase transition, achieved through collective effects in many-body interacting systems [15, 33, 38, 40–42]. By focusing on the resulting energy-level structure rather than delving into the intricate interactions within many-body systems, our model succinctly and intuitively demonstrates how collective effects enhance the performance of heat engines. Our approach will open up new avenues for optimizing heat engines, going beyond the conventional pursuit of optimal cycle control scheme [11, 43–45] by introducing the concept of designing optimal internal structure for the engines' working substances.

Acknowledgments.— We thank Simone Pigolotti for comments on a preliminary version of this manuscript. S.L. thanks the JSPS Strategic Fellowship for support under grant No. GR22106. S.L. and P.D.L.R. thank the Swiss National Science Foundation for support under grant 200020_178763. Y. H. Ma thanks the National Natural Science Foundation of China for support under grant No. 12305037 and the Fundamental Research Funds for the Central Universities for support under grant No. 2233100024.

* shiling.liang@epfl.ch

† yhma@bnu.edu.cn

- [1] H. B. Callen, *Thermodynamics and an Introduction to Thermostatistics* (John Wiley & sons, 1991).
- [2] I. Novikov, The efficiency of atomic power stations (a review), *Journal of Nuclear Energy* (1954) **7**, 125 (1958).
- [3] F. L. Curzon and B. Ahlborn, Efficiency of a Carnot engine at maximum power output, *American Journal of Physics* **43**, 22 (1975).
- [4] C. Van den Broeck, Thermodynamic Efficiency at Maximum Power, *Physical Review Letters* **95**, 190602 (2005).
- [5] T. Schmiedl and U. Seifert, Efficiency of molecular motors at maximum power, *Europhysics Letters* **83**, 30005 (2008).
- [6] Z. C. Tu, Efficiency at maximum power of Feynman's ratchet as a heat engine, *Journal of Physics A: Mathematical and Theoretical* **41**, 312003 (2008).
- [7] M. Esposito, R. Kawai, K. Lindenberg, and C. Van den Broeck, Efficiency at Maximum Power of Low-Dissipation Carnot Engines, *Physical Review Letters* **105**, 150603 (2010).
- [8] L. Chen and Z. Yan, The effect of heat-transfer law on performance of a two-heat-source endoreversible cycle, *The Journal of Chemical Physics* **90**, 3740 (1989).
- [9] V. Holubec and A. Ryabov, Maximum efficiency of low-dissipation heat engines at arbitrary power, *Journal of Statistical Mechanics: Theory and Experiment* **2016**, 073204 (2016).
- [10] Y.-H. Ma, D. Xu, H. Dong, and C.-P. Sun, Universal constraint for efficiency and power of a low-dissipation heat engine, *Physical Review E* **98**, 042112 (2018).
- [11] H. Yuan, Y.-H. Ma, and C. P. Sun, Optimizing thermodynamic cycles with two finite-sized reservoirs, *Physical Review E* **105**, L022101 (2022).
- [12] R.-X. Zhai, F.-M. Cui, Y.-H. Ma, C. Sun, and H. Dong, Experimental test of power-efficiency trade-off in a finite-time carnot cycle, *Physical Review E* **107**, L042101 (2023).
- [13] B. Andresen, Current trends in finite-time thermodynamics, *Angewandte Chemie International Edition* **50**, 2690 (2011).
- [14] Z.-C. Tu, Abstract models for heat engines, *Frontiers of Physics* **16**, 1 (2021).
- [15] M. Campisi and R. Fazio, The power of a critical heat engine, *Nature Communications* **7**, 11895 (2016).
- [16] M. Poletti and M. Esposito, Carnot efficiency at divergent power output, *EPL (Europhysics Letters)* **118**, 40003 (2017).
- [17] J. S. Lee and H. Park, Carnot efficiency is reachable in an irreversible process, *Scientific Reports* **7**, 10725 (2017).
- [18] P. Abiuso and M. Perarnau-Llobet, Optimal Cycles for Low-Dissipation Heat Engines, *Physical Review Letters* **124**, 110606 (2020).
- [19] U. Seifert, Efficiency of Autonomous Soft Nanomachines at Maximum Power, *Physical Review Letters* **106**, 020601 (2011).
- [20] A. E. Allahverdyan, K. V. Hovhannisyan, A. V. Melkikh, and S. G. Gevorkian, Carnot Cycle at Finite Power: Attainability of Maximal Efficiency, *Physical Review Letters* **111**, 050601 (2013).
- [21] Z. C. Tu, Recent advance on the efficiency at maximum power of heat engines, *Chinese Physics B* **21**, 020513 (2012).
- [22] C. Maffi, M. Baiesi, L. Casetti, F. Piazza, and P. De Los Rios, First-order coil-globule transition driven by vibrational entropy, *Nature Communications* **3**, 1065 (2012).
- [23] S. Liang, D. M. Busiello, and P. D. L. Rios, Emergent thermophoretic behavior in chemical reaction systems, *New Journal of Physics* **24**, 123006 (2022).
- [24] A. V. Dass, T. Georgelin, F. Westall, F. Foucher, P. De Los Rios, D. M. Busiello, S. Liang, and F. Piazza, Equilibrium and non-equilibrium furanose selection in the ribose isomerisation network, *Nature Communica-*

- tions **12**, 2749 (2021).
- [25] C. Maes, Local detailed balance, SciPost Physics Lecture Notes , 32 (2021).
- [26] L. Peliti and S. Pigolotti, *Stochastic Thermodynamics: An Introduction* (Princeton University Press, 2021).
- [27] See supplemental materials for analytical derivations and mathematical details of the stationary state in Sec. I, quality of the Otto cycle in Sec. II, power-efficiency trade-off in Sec. III, and the limit of EMP in Sec. IV.
- [28] M. Esposito, Stochastic thermodynamics under coarse graining, Physical Review E **85**, 041125 (2012).
- [29] U. Seifert, Stochastic thermodynamics of single enzymes and molecular motors, The European Physical Journal E **34**, 26 (2011).
- [30] F. L. Curzon and B. Ahlborn, Efficiency of a Carnot engine at maximum power output, American Journal of Physics **43**, 22 (1975).
- [31] R. Kawai, J. M. R. Parrondo, and C. V. den Broeck, Dissipation: The Phase-Space Perspective, Physical Review Letters **98**, 080602 (2007).
- [32] J. M. R. Parrondo, J. M. Horowitz, and T. Sagawa, Thermodynamics of information, Nature Physics **11**, 131 (2015).
- [33] Y.-H. Ma, S.-H. Su, and C.-P. Sun, Quantum thermodynamic cycle with quantum phase transition, Physical Review E **96**, 022143 (2017).
- [34] N. Shiraishi, K. Saito, and H. Tasaki, Universal Trade-Off Relation between Power and Efficiency for Heat Engines, Physical Review Letters **117**, 190601 (2016).
- [35] This finding leaves an open question: Does a tight analytical tradeoff between power and efficiency exist throughout the entire range of $\tilde{\eta}$? We have attempted to find it but have not been successful so far. The asymptotic expressions in Eq. (13) at both ends of $\tilde{\eta}$ can serve as a good approximation for the complete tradeoff relation in the large- s regime.
- [36] I. A. Martínez, É. Roldán, L. Dinis, D. Petrov, J. M. Parrondo, and R. A. Rica, Brownian carnot engine, Nature physics **12**, 67 (2016).
- [37] Y.-H. Ma, R.-X. Zhai, J. Chen, C. Sun, and H. Dong, Experimental test of the $1/\tau$ -scaling entropy generation in finite-time thermodynamics, Physical Review Letters **125**, 210601 (2020).
- [38] A. Rolandi, P. Abiuso, and M. Perarnau-Llobet, Collective advantages in finite-time thermodynamics, Physical Review Letters **131**, 210401 (2023).
- [39] S. H. Lee, J. Um, and H. Park, Nonuniversality of heat-engine efficiency at maximum power, Physical Review E **98**, 052137 (2018).
- [40] H. Vroylandt, M. Esposito, and G. Verley, Collective effects enhancing power and efficiency, Europhysics Letters **120**, 30009 (2018).
- [41] T. Herpich, J. Thingna, and M. Esposito, Collective Power: Minimal Model for Thermodynamics of Nonequilibrium Phase Transitions, Physical Review X **8**, 031056 (2018).
- [42] F. S. Filho, G. A. L. Forão, D. M. Busiello, B. Cleuren, and C. E. Fiore, Powerful ordered collective heat engines (2023), arxiv:2301.06591 [cond-mat, physics:nlin, physics:quant-ph].
- [43] Y.-H. Ma, D. Xu, H. Dong, and C.-P. Sun, Optimal operating protocol to achieve efficiency at maximum power of heat engines, Physical Review E **98**, 022133 (2018).
- [44] A. G. Frim and M. R. DeWeese, Geometric bound on the efficiency of irreversible thermodynamic cycles, Physical Review Letters **128**, 230601 (2022).
- [45] Y. Chen, J.-F. Chen, Z. Fei, and H. Quan, Microscopic theory of the curzon-ahlborn heat engine based on a brownian particle, Physical Review E **106**, 024105 (2022).

Supplemental Materials for: “A Minimal Model for Carnot Efficiency at Maximum Power”

Shiling Liang (梁师翎)^{1,2,*} Yu-Han Ma,^{3,4,†} Daniel Maria Busiello,⁵ and Paolo De Los Rios^{1,6}

¹*Institute of Physics, School of Basic Sciences, École Polytechnique Fédérale de Lausanne (EPFL), 1015 Lausanne, Switzerland*

²*Biological Complexity Unit, Okinawa Institute of Science and
Technology Graduate University, Onna, Okinawa 904-0495, Japan*

³*Department of Physics, Beijing Normal University, Beijing, 100875, China*

⁴*Graduate School of China Academy of Engineering Physics,
No. 10 Xibeiwang East Road, Haidian District, Beijing, 100193, China*

⁵*Max Planck Institute for the Physics of Complex Systems, 01187 Dresden, Germany*

⁶*Institute of Bioengineering, School of Life Sciences,
École Polytechnique Fédérale de Lausanne (EPFL), 1015 Lausanne, Switzerland*

I. THE STATIONARY STATE

For the master equation of the biochemical engine

$$\begin{aligned}\frac{d}{dt}p_u &= (k_{h-} + k_{c-})p_v - (k_{h+} + k_{c+})p_u, \\ \frac{d}{dt}p_v &= (k_{h+} + k_{c+})p_u - (k_{h-} + k_{c-})p_v,\end{aligned}\tag{S1}$$

its stationary distribution satisfies

$$p_v^{\text{ss}} = \frac{k_{h+} + k_{c+}}{k_{h-} + k_{c-}} p_u^{\text{ss}},\tag{S2}$$

with the normalization condition $p_u^{\text{ss}} + p_v^{\text{ss}} = 1$, one can find the stationary distribution of the probability on the state U as

$$p_u^{\text{ss}} = \frac{k_{h-} + k_{c-}}{k_{h+} + k_{h-} + k_{c+} + k_{c-}} = \frac{k_h}{k_c + k_h} \underbrace{\frac{k_{h-}}{k_h}}_{\pi_u^h} + \frac{k_c}{k_c + k_h} \underbrace{\frac{k_{c-}}{k_c}}_{\pi_u^c},\tag{S3}$$

where we define the characteristic rate in two reservoirs as $k_h = k_{h-} + k_{h+}$ and $k_c = k_{c-} + k_{c+}$. The stationary value of p_v^{ss} can be obtained in the same fashion. The steady-state flux is

$$\begin{aligned}J^{\text{ss}} &= k_{h+}p_u^{\text{ss}} - k_{h-}p_v^{\text{ss}} \\ &= \frac{k_{h+}(k_{h-} + k_{c-}) - k_{h-}(k_{h+} + k_{c+})}{2(k_c + k_h)} \\ &= \frac{k_c k_h}{(k_c + k_h)} \left(\frac{k_{h+}k_{c-}}{k_c k_h} - \frac{k_{h-}k_{c+}}{k_c k_h} \right) \\ &= \frac{k_c k_h}{(k_c + k_h)} \left(\frac{k_{h+}}{k_h} \left(1 - \frac{k_{c+}}{k_c} \right) - \left(1 - \frac{k_{h+}}{k_h} \right) \frac{k_{c+}}{k_c} \right) \\ &= \frac{k_c k_h}{(k_c + k_h)} \left(\frac{k_{h+}}{k_h} - \frac{k_{c-}}{k_c} \right) \\ &= \frac{1}{\tau_h + \tau_c} (\pi_v^h - \pi_v^c).\end{aligned}\tag{S4}$$

where we define the two timescales of transitions in hot and cold reservoirs as $\tau_h = k_h^{-1}$ and $\tau_c = k_c^{-1}$.

* shiling.liang@epfl.ch

† yhma@bnu.edu.cn

II. QUALITY OF THE OTTO CYCLE

The extractable after the two Otto quenches are the remained amount of information encoded in the non-equilibrium distributions, which can be computed as the non-equilibrium free energy difference

$$\Delta\mathcal{F}_{cd} = \epsilon_h(\pi_v^c - \pi_v^h) - T_h(S_c - S_h) = -\epsilon_h\Delta\pi + T_h\Delta S, \quad (\text{S5})$$

$$\Delta\mathcal{F}_{ab} = \epsilon_c(\pi_v^h - \pi_v^c) - T_c(S_h - S_c) = \epsilon_c\Delta\pi - T_c\Delta S. \quad (\text{S6})$$

When we calculate the entropy change, we need to be aware that the system is coarse-grained so that some system entropy is hidden in the degeneracy. For a give coarse-grained 2-state distribution (p_u, p_v) , the exact entropy is

$$S(p_u, p_v) = -p_u \ln p_u - p_v \ln p_v + \underbrace{p_u \ln n_u + p_v \ln n_v}_{p_v s + \ln n_u}. \quad (\text{S7})$$

We denote the first part as $S_0 = -p_u \ln u - p_v \ln v$. Therefore we can find that slow-work

$$W_{\text{slow}} = -\Delta\epsilon\Delta\pi + \Delta T\Delta S_0 + \Delta\pi s\Delta T, \quad (\text{S8})$$

and fast-work as

$$W_{\text{fast}} = (\epsilon_h - \epsilon_c)(\pi_v^h - \pi_v^c) = \Delta\epsilon\Delta\pi. \quad (\text{S9})$$

The quality which quantifies the fraction of fast-work is given by

$$\mathcal{Q} \equiv \frac{W_{\text{fast}}}{W_{\text{fast}} + W_{\text{slow}}} = \frac{\Delta\epsilon\Delta\pi}{\Delta\pi s\Delta T + \Delta T\Delta S_0}. \quad (\text{S10})$$

When s is large, the coarse-grained stats contribute the most of entropic change thus we can drop the ΔS_0 term. And the quality factor is given by

$$\lim_{s \gg 1} \mathcal{Q} = \frac{\Delta\epsilon}{s\Delta T} = \frac{\bar{\epsilon}_h - \bar{\epsilon}_c}{T_h - T_c}. \quad (\text{S11})$$

III. POWER-EFFICIENCY TRADE-OFF RELATION

The general Power-efficiency trade-off with different s is numerically plotted in Fig. ??b of the main text. It is clearly seen in this figure that for an arbitrary given power, the maximum achievable efficiency increases with s . Hence, we reasonably speculate that the upper branch of the trade-off will become a plateau ($\eta = \eta_C$) at the thermodynamic limit of $s \rightarrow \infty$. This means that maximum power and maximum efficiency can be achieved simultaneously. To analytically prove this result, we focus on this trade-off relation under two limits of η . The normalized efficiency $\tilde{\eta} \equiv \eta/\eta_C$ will be used below. As demonstrated in the main text, the power of biochemical engine can be written as

$$P = \tilde{\eta}\epsilon_h\tau^{-1} \left(\frac{\eta_C}{e^{\epsilon_h - s} + 1} - \frac{\eta_C}{e^{\frac{\epsilon_h(1-\tilde{\eta}\eta_C)}{1-\eta_C} - s} + 1} \right) \quad (\text{S12})$$

where we use $k_B T_h = 1$ as the reference energy.

a. $\tilde{\eta} \rightarrow 1$ limit In this limit, we expand the power in Eq. (S12) in terms of $\sigma \equiv (1 - \tilde{\eta})$ up to the first-order term as

$$P = \frac{\eta_C^2 \epsilon_h^2 e^{\epsilon_h - s}}{(1 - \eta_C)(e^{\epsilon_h - s} + 1)^2} \sigma + \mathcal{O}(\sigma^2), \quad (\text{S13})$$

where we use the high-temperature rescaled energy level $\epsilon_h \equiv \epsilon_h/T_h$ to simplify the expression. The trade-off curve is with the maximized linear coefficient. For fixed entropy difference, we optimize the coefficient with respect to ϵ_h , namely

$$\frac{d}{d\varepsilon_h} \left(\frac{\eta_C^2 \varepsilon_h^2 e^{\varepsilon_h - s}}{(1 - \eta_C)(e^{\varepsilon_h - s} + 1)^2} \right) = 0. \quad (\text{S14})$$

The above equality leads to

$$e^{\varepsilon_h - s} = \frac{\varepsilon_h + 2}{\varepsilon_h - 2}. \quad (\text{S15})$$

In the large degeneracy regime ($s \gg 1$), the solution of the above equation is approximately $\varepsilon_h = s$, substituting which back to Eq. (S13) yields

$$\lim_{\tilde{\eta} \rightarrow 1} P \simeq \frac{s^2 \eta_C^2}{4(1 - \eta_C)} (1 - \tilde{\eta}) \quad (\text{S16})$$

b. $\tilde{\eta} \rightarrow 0$ limit In this limit, we can expand the power in Eq. (S12) with respect to $\tilde{\eta}$ to get the first order term as

$$P = \eta_C \varepsilon_h \left(\frac{1}{e^{\varepsilon_h - s} + 1} - \frac{1}{e^{\frac{\varepsilon_h}{1 - \eta_C} - s} + 1} \right) \tilde{\eta} + \mathcal{O}(\tilde{\eta}^2). \quad (\text{S17})$$

With the definition $x \equiv \varepsilon_h - s$, Eq. (S17) is re-written as

$$P \simeq \eta_C (s + x) \left(\frac{1}{e^x + 1} - \frac{1}{e^{\frac{x + \eta_C s}{1 - \eta_C} + 1}} \right). \quad (\text{S18})$$

Optimizing P with respect to x , namely,

$$\frac{dP}{dx} = \eta_C \frac{d}{dx} \left[(s + x) \left(\frac{1}{e^x + 1} - \frac{1}{e^{\frac{x + \eta_C s}{1 - \eta_C} + 1}} \right) \right] = 0, \quad (\text{S19})$$

which leads to

$$\frac{1}{e^x + 1} - \frac{1}{e^{\frac{x + \eta_C s}{1 - \eta_C} + 1}} + (s + x) \left[\frac{-e^x}{(e^x + 1)^2} - \frac{-e^{\frac{x + \eta_C s}{1 - \eta_C}}}{(1 - \eta_C) \left(e^{\frac{x + \eta_C s}{1 - \eta_C} + 1} \right)^2} \right] = 0. \quad (\text{S20})$$

We also focus on the large degeneracy regime ($s \gg 1$) in which we intuitively guess that the solution of the above equality, i.e. $x = x^*$ satisfies

$$1 \ll |x^*| \ll s, \quad (\text{S21})$$

such that we have

$$\frac{1}{e^{\frac{x + \eta_C s}{1 - \eta_C} + 1}} \approx 0, \quad \frac{e^{\frac{x + \eta_C s}{1 - \eta_C}}}{(1 - \eta_C) \left(e^{\frac{x + \eta_C s}{1 - \eta_C} + 1} \right)^2} \approx 0, \quad s + x \approx s \quad (\text{S22})$$

up to the first order of s . Then, Eq. (S20) is approximated as

$$\frac{1}{e^x + 1} - \frac{s e^x}{(e^x + 1)^2} = 0. \quad (\text{S23})$$

The solution of the above equality is $e^x = 1/(s - 1)$, namely

$$x^* = -\ln(s - 1) \simeq -\ln s. \quad (\text{S24})$$

This solution is consistent with the assumption in Eq. (S21). Finally, we obtain the optimal ε_h in the small $\tilde{\eta}$ and large s as

$$\varepsilon_h = \varepsilon_h^* = s - \ln s. \quad (\text{S25})$$

Substitute it into Eq. (S17) and take the large s limit further simplify the coefficient, we get

$$\lim_{\tilde{\eta} \rightarrow 0} P \simeq \frac{s(s - \ln s)\eta_C}{s + 1} \tilde{\eta}. \quad (\text{S26})$$

These two linear expansion gives an upper bound of the power-efficiency trade-off curve. The upper bounds of the re-scaled efficiency at maximum power and maximum power are given by the intersection of these two lines, denoted as $(\tilde{\eta}', P')$, which can be simply obtained as

$$\tilde{\eta}' \simeq \frac{(s + 1)\eta_C}{(s - 3)\eta_C + 4} \simeq 1 - \frac{4(1 - \eta_C)}{\eta_C} s^{-1}, \quad (\text{S27})$$

and $P' \simeq \eta_C s$, respectively. Note that the maximum power increases linearly with s while the EMP approaches to Carnot efficiency in inverse proportion to s . This means that increasing the degeneracy of the system can improve the power and maximum power efficiency of the engine at the same time, which is a perfect advantage.

Moreover, the numerical evidences suggest that, besides $\tilde{\eta} = 1$, the linear expansion in Eq. (S26) can be a good approximation of the power-efficiency tradeoff in the interval $0 \leq \tilde{\eta} < 1$. In this sense, the normalized approximate trade-off becomes

$$\tilde{P} \equiv \frac{P}{P'} \leq \left(1 - \frac{\ln s}{s}\right) \tilde{\eta}. \quad (\text{S28})$$

Geometrically, the approximate tradeoff relation becomes an isosceles right triangle in the normalized power-efficiency parametric space since $\lim_{s \rightarrow \infty} d\tilde{P}/d\tilde{\eta} = 1$. This is intuitively reflected in the tradeoff curve associated with $s = 10^3$ in Fig. ??b of the main text.

IV. EMP IN THE LIMITS $\eta_C \rightarrow 0$ AND $\eta_C s \rightarrow 0$

It follows from Eq. (S12) that

$$P \propto \eta\theta \left[\frac{1}{1 + e^{\theta(1-\eta_C)-s}} - \frac{1}{1 + e^{\theta(1-\eta)-s}} \right] = \eta\theta \left[\frac{1}{1 + e^{\theta-s-\eta_C\theta}} - \frac{1}{1 + e^{\theta-s-\eta\theta}} \right], \quad (\text{S29})$$

where $\theta = \varepsilon_h \beta_c$. In the limits of $\eta_C \rightarrow 0$ and $\eta_C s \rightarrow 0$, it is naturally to assume that $\eta\theta \leq \eta_C\theta \ll 1$, such that

$$P \propto \eta\theta \left[\frac{1}{1 + e^{\theta-s}(1 - \eta_C\theta)} - \frac{1}{1 + e^{\theta-s-\eta\theta}(1 - \eta\theta)} \right] \quad (\text{S30})$$

$$\simeq \frac{\eta\theta [e^{\theta-s}(1 - \eta\theta) - e^{\theta-s}(1 - \eta_C\theta)]}{[1 + e^{\theta-s}(1 - \eta_C\theta)][1 + e^{\theta-s-\eta\theta}(1 - \eta\theta)]} \quad (\text{S31})$$

$$\simeq \frac{e^{\theta-s}\theta^2\eta(\eta_C - \eta)}{(1 + e^{\theta-s})^2}. \quad (\text{S32})$$

We optimize P with respect to η directly gives

$$\frac{\partial P}{\partial \eta} = 0 \rightarrow \eta_C - 2\eta = 0, \quad (\text{S33})$$

which indicates that the efficiency at maximum power is

$$\lim_{\eta_C \rightarrow 0} \eta_{\text{MP}} = \frac{\eta_C}{2} \quad (\text{S34})$$